© 2021. Published by The Company of Biologists Ltd | Development (2021) 148, dev197020. doi:10.1242/dev.197020

RESEARCH ARTICLE

Lrig1 and Lrig3 cooperate to control Ret receptor signaling, sensory axonal growth and epidermal innervation

Ana Paula De Vincenti[1,*], Fernando C. Alsina[1,*], Facundo Ferrero Restelli[1], Håkan Hedman[2], Fernanda Ledda[1,3] and Gustavo Paratcha[1,‡]

ABSTRACT

Negative feedback loops represent a regulatory mechanism that guarantees that signaling thresholds are compatible with a physiological response. Previously, we established that Lrig1 acts through this mechanism to inhibit Ret activity. However, it is unclear whether other Lrig family members play similar roles. Here, we show that Lrig1 and Lrig3 are co-expressed in Ret-positive mouse dorsal root ganglion (DRG) neurons. Lrig3, like Lrig1, interacts with Ret and inhibits GDNF/Ret signaling. Treatment of DRG neurons with GDNF ligands induces a significant increase in the expression of Lrig1 and Lrig3. Our findings show that, whereas a single deletion of either Lrig1 or Lrig3 fails to promote Ret-mediated axonal growth, haploinsufficiency of Lrig1 in Lrig3 mutants significantly potentiates Ret signaling and axonal growth of DRG neurons in response to GDNF ligands. We observe that Lrig1 and Lrig3 act redundantly to ensure proper cutaneous innervation of nonpeptidergic axons and behavioral sensitivity to cold, which correlates with a significant increase in the expression of the cold-responsive channel TrpA1. Together, our findings provide insights into the *in vivo* functions through which Lrig genes control morphology, connectivity and function in sensory neurons.

KEY WORDS: Lrig family members, GDNF, GFRα, Ret, Dorsal root ganglia (DRG), Cutaneous sensory innervation and nociceptive neurons, Mouse

INTRODUCTION

The establishment of precise neuronal circuits during development is essential for the proper execution of sensory processing and perception. Dorsal root ganglion (DRG) neurons form a circuit that conveys signals from peripheral sensory organs to the spinal cord. DRG sensory neuron subtypes can be classified by the expression of different neurotrophic factor receptors. These receptors are crucial for peripheral axonal growth and branching, target tissue innervation, and neuronal survival as well as the expression of several ion channels and receptors that define the nociceptive, mechanoreceptive and proprioceptive modalities of the different subtypes of sensory neurons (Marmigere and Ernfors, 2007).

Nociceptive neurons can be further classified into two populations. One expresses the NGF receptor TrkA (Ntrk1) together with the peptidergic markers calcitonin-gene related peptide (CGRP) and substance P (Tac1) (Lallemend and Ernfors, 2012). The second population, termed nonpeptidergic, expresses the glial cell line-derived neurotrophic factor (GDNF) family ligands (GFLs) receptor Ret, a tyrosine kinase transmembrane molecule that is activated by GDNF, neurturin (NRTN), artemin (ARTN) and persephin (PSPN) (Airaksinen and Saarma, 2002). GFLs promote survival and differentiation of motor neurons (Henderson et al., 1994; Li et al., 1995; Oppenheim et al., 1995) and different populations of sympathetic and sensory neurons (Airaksinen et al., 1999; Paratcha and Ledda, 2008) through the activation of a dual receptor system formed by the glycosyl-phosphatidyl inositol (GPI)-linked GFRα co-receptor, specialized in ligand binding (Jing et al., 1996; Treanor et al., 1996), and the receptor tyrosine kinase Ret, specialized in transmembrane signaling (Durbec et al., 1996; Trupp et al., 1996). In this receptor system, GFLs could not bind and activate Ret in the absence of GFRα co-receptor, indicating that both receptor subunits are required for GDNF signaling.

Previous studies of genetically modified mice have demonstrated that GFL-induced Ret signaling is important for cell migration, axonal growth and cell survival during peripheral nervous system development (Fundin et al., 1999; Kramer et al., 2006).

Conditional deletion of Ret in sensory neurons has been performed to analyze its physiological contribution to nonpeptidergic nociceptive neuron development during postnatal stages (Luo et al., 2007). This study established that Ret signaling is crucial for acquisition of several features of the nonpeptidergic neuronal phenotype, including innervation of the epidermis, control of normal neuronal size and postnatal extinction of TrkA. Furthermore, overexpression of GDNF, NRTN or ARTN in mice skin resulted in epidermal hyperinnervation (Elitt et al., 2006; Wang et al., 2013; Zwick et al., 2002) and altered thermal sensitivity.

Recent findings indicate that neurotrophic factor receptors associate with diverse leucine-rich repeat (LRR)-containing proteins to modulate their signaling outputs (Alsina et al., 2016; Ledda et al., 2008; Mandai et al., 2009; Meabon et al., 2015; Song et al., 2015). Several LRR protein family members have been detected in non-overlapping subsets of sensory and motor neurons, raising the possibility that different LRR transmembrane proteins regulate neurotrophic factor receptor activation in specific populations of developing sensory neurons (Ledda and Paratcha, 2016; Mandai et al., 2009).

In particular, the leucine-rich repeats and immunoglobulin-like domains (Lrig) family of transmembrane proteins contains three vertebrate members (Lrig1, Lrig2 and Lrig3) (Dolan et al., 2007). Although the physiological contribution of Lrigs is not completely

[1]Laboratorio de Neurociencia Molecular y Celular, Instituto de Biología Celular y Neurociencias (IBCN)-CONICET-UBA, Facultad de Medicina, Universidad de Buenos Aires (UBA), Buenos Aires, CP1121, Argentina. [2]Oncology Research Laboratory, Department of Radiation Sciences, Umeå University, Umeå, 901 87, Sweden. [3]Fundación Instituto Leloir, Instituto de Investigaciones Bioquímicas de Buenos Aires, Buenos Aires, C1405, Argentina.
*These authors contributed equally to this work

‡Author for correspondence (gparatcha@fmed.uba.ar)

A.P.D., 0000-0003-2051-1169; F.C.A., 0000-0002-6304-7688; F.F., 0000-0002-1609-0130; H.H., 0000-0001-6891-6996; F.L., 0000-0002-9769-6926; G.P., 0000-0002-0804-4433

Handling Editor: Paola Arlotta
Received 16 September 2020; Accepted 5 July 2021

Development (2021) 148, dev197020. doi:10.1242/dev.197020

known yet, biological evidence shows that during development Lrig genes have both independent and redundant functions (Del Rio et al., 2013). Previously, our group identified Lrig1 as an endogenous inhibitor of the GDNF receptor Ret (Ledda et al., 2008). Lrig1 directly associates with Ret and negatively regulates Ret signaling and axonal growth of sympathetic neurons in response to GDNF, through a mechanism that involves blockade of GDNF binding to Ret (Ledda et al., 2008). However, the contribution of other Lrig family members for GDNF-induced Ret signaling and biology remains to be determined.

Notably, Lrig1 and Lrig3 proteins are closely related. Both proteins have a highly conserved extracellular domain, which suggests that they could interact with common receptor partners (Abraira et al., 2008; Guo et al., 2004). Lrig1 and Lrig3 also show partially overlapping patterns of expression in different tissues throughout development and exhibit common functions both *in vitro* and *in vivo* (Abraira et al., 2008; Del Rio et al., 2013; Homma et al., 2009) although Lrig1 and Lrig3 have also been suggested to oppose each other (Rafidi et al., 2013). Functional analysis of Lrig2 suggests that this other member of the family has acquired independent functions. At the molecular level, only Lrig1 and Lrig3 have been reported to act as receptor tyrosine kinase inhibitors (Alsina et al., 2016; Guo et al., 2015; Gur et al., 2004; Laederich et al., 2004; Ledda et al., 2008; Shattuck et al., 2007). It is noteworthy that previous evidence has indicated that Lrig1 and Lrig3 function as tumor suppressors, regulating glioblastoma progression and restricting EGFR signaling (Guo et al., 2015).

Based on this evidence, we decided to explore the role of Lrig3 in GDNF-induced Ret signaling and analyze a possible biological contribution of Lrig1 and Lrig3 in Ret-mediated trophic events, such as axonal growth of DRG sensory neurons, cutaneous sensory innervation of nonpeptidergic neurons and thermal responsiveness. Our findings indicate that Lrig1 and Lrig3 function redundantly by inhibiting Ret signaling and neurite outgrowth of sensory neurons to safeguard proper axonal development and connectivity.

RESULTS

Lrig3 interacts with Ret and restricts GDNF-induced Ret tyrosine kinase activation, downstream signaling and neurite outgrowth

Previous studies from our laboratory established that Lrig1 is an endogenous interactor of Ret, and that Lrig1/Ret association restricts GDNF binding, Ret receptor tyrosine phosphorylation and Erk1/2 (Mapk3/1) signaling in response to GDNF (Ledda et al., 2008). To study whether Lrig3 might also regulate GDNF/Ret signaling, we first examined its ability to interact with Ret receptor. To explore this possibility, we performed a co-immunoprecipitation assay in HEK-293T cells transfected with Flag-Lrig3 in the absence or in the presence of Ret. As we reported previously for Lrig1, Ret specifically co-immunoprecipitated with either Flag-Lrig1 or Flag-Lrig3 constructs (Fig. 1A).

Then, we evaluated whether overexpression of Lrig3 might regulate GDNF-induced Ret receptor tyrosine phosphorylation, Erk1/2 and Akt activation in the motor neuron cell line MN1, which expresses endogenous levels of GDNF receptors, Ret and GFRα1. For these experiments, control and Lrig3-overexpressing cells were serum-starved and treated with GDNF for 15 min. The level of Ret activation was determined by immunoprecipitation with specific antibodies followed by immunoblotting with anti-phosphotyrosine antibodies. Similarly to Lrig1, MN1 cells overexpressing Lrig3 showed a significant reduction in GDNF-induced Ret tyrosine phosphorylation compared with control cells (Fig. 1B,C).

To evaluate whether Lrig3 could regulate the Erk/MAPK pathway downstream of Ret, we transiently co-transfected HA-Erk2/MAPK plasmid with control, or Flag-Lrig3 constructs into MN1 cells. After 36 h, cells were serum-starved and stimulated with or without GDNF for 15 min. The level of Erk2 activation was examined by HA immunoprecipitation followed by immunoblotting with anti-phospho Erk1/2 antibodies. MN1 cells overexpressing Flag-Lrig3 showed a significant reduction in the levels of Erk2/MAPK activation in response to GDNF (Fig. 1D,E). To evaluate Akt activity, MN1 cells were transfected with empty vector or Flag-Lrig3 constructs. After starving, the cells were stimulated with GDNF for 10 min, and the activity of Akt was evaluated by immunoblotting using a phospho-specific antibody (Fig. S1). In this experiment, we observed that Lrig3 was able to inhibit Akt activation in response to GDNF (Fig. S1). These results indicate that Lrig3 associates with Ret and inhibits its downstream signaling.

In a previous study, we demonstrated that Lrig1 inhibits neurite outgrowth of MN1 cells treated with GDNF and the soluble form of the GPI co-receptor, GFRα1-Fc, which potentiates the effects of GDNF (Ledda et al., 2008). Based on this evidence, we examined whether Lrig3 may also attenuate Ret-dependent morphological differentiation of MN1 cells. For these experiments, MN1 cells were transfected with either control or Lrig3 vectors together with a vector expressing GFP. Whereas GDNF and soluble GFRα1 induced a robust neuronal differentiation of control transfected MN1 cells, which was characterized by the development of long neurites, Lrig3-overexpressing MN1 cells failed to morphologically differentiate in response to GDNF and GFRα1-Fc (Fig. 1F,G).

Altogether, these results indicate that, similarly to Lrig1, Lrig3 is able to interact with Ret and block GDNF-induced Ret activation, downstream signaling and neurite outgrowth.

Lrig1 and Lrig3 are highly co-expressed with Ret in DRG and are induced by GDNF ligands in sensory neurons

To explore whether Lrig1 and Lrig3 could be involved in the control of Ret function *in vivo*, we examined their expression by RT-PCR and immunofluorescence in transverse sections of lumbar DRG at different developmental stages. Higher *Lrig1* and *Lrig3* mRNA expression was detected at late embryonic and early postnatal developmental stages, a period in which a progressive increase in *Ret* expression occurs in nociceptive DRG neurons in mouse (Fig. 2A) (Molliver et al., 1997).

Immunofluorescence staining revealed a striking co-expression of Lrig1 with Ret (≈79%) and Lrig3 with Ret (≈91%), in lumbar sensory ganglia of newborn mice (Fig. 2B-D). A high level of colocalization was also observed at P15, when the segregation of $TrkA^{+}/Ret^{-}$ and $TrkA^{-}/Ret^{+}$ populations is nearly complete, and at adult stages of mouse DRG development. This result indicates that most Ret-positive DRG neurons express Lrig1, Lrig3 or both at all the analyzed stages. In agreement with the *in vivo* results, the staining of primary DRG dissociated neurons revealed a striking co-expression of Lrig1 and Lrig3 with the GDNF receptor Ret (Fig. S2). The specificity of the Lrig1 antibody has been previously reported (Alsina et al., 2016) and Lrig3 was validated by immunofluorescence and immunoblotting in tissue and extracts obtained from Lrig3-deficient mice (Fig. S3).

Previous evidence has demonstrated the importance of negative-feedback regulation of neurotrophic factor receptor function as a mechanism that ensures that signaling thresholds compatible with the induction of a physiological response (Alsina et al., 2012; Gur et al., 2004; Ledda et al., 2008). A common feature of regulation by negative-feedback loops is ligand-dependent induction of receptor

Development (2021) 148, dev197020. doi:10.1242/dev.197020

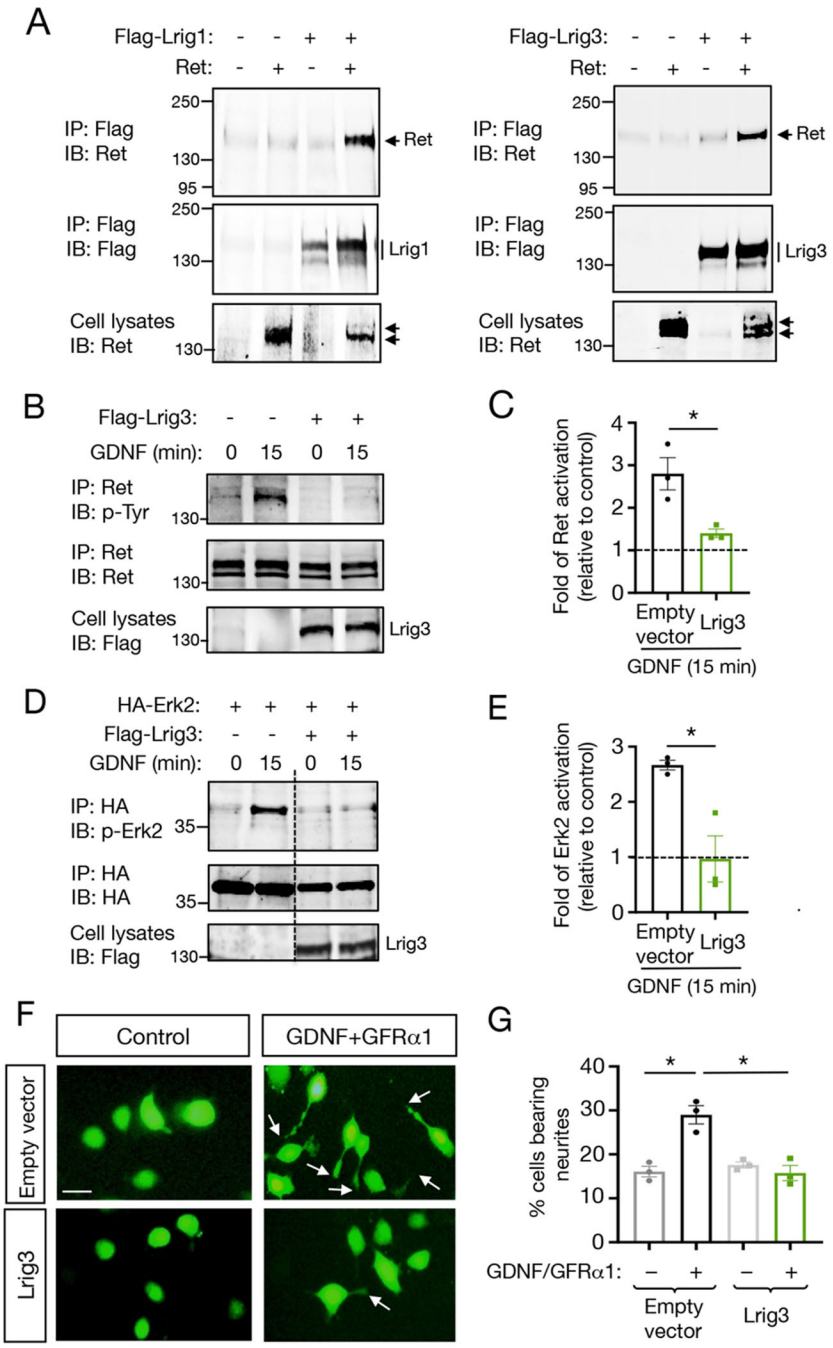

Fig. 1. Lrig3 interacts with Ret and restricts GDNF-induced Ret receptor tyrosine kinase phosphorylation, MAPK activation and neurite outgrowth. (A) Co-immunoprecipitation between either Flag-tagged Lrig1 or Flag-tagged Lrig3 and Ret overexpressed in HEK-293T cells. Cell extracts were analyzed by immunoprecipitation (IP) with anti-Flag antibodies followed by immunoblot (IB) with antibodies against Ret. The same blot was re-probed with anti-Flag antibodies. Expression of Ret in total cell lysates is also shown. (B) Ret tyrosine phosphorylation in control and MN1 cells overexpressing Flag-Lrig3 and treated with GDNF (50 ng/ml) as indicated. Total lysates were immunoprecipitated with anti-Ret antibodies followed by immunoblot with antibodies against phosphotyrosine (p-Tyr). The same blot was re-probed with anti-Ret antibodies. Expression of Flag-Lrig3 in total cell lysates is also shown. (C) Bar graph showing quantification of Ret phosphorylation in control versus MN1 cells overexpressing Flag-Lrig3. Results are presented as fold change of Ret activation relative to control untreated samples (dashed line). Data are mean±s.e.m. of n=3 independent experiments. *P<0.05, two-tailed Student's t-test. (D) Erk2 activation in cell extracts prepared from MN1 cells co-transfected with either empty vector or Flag-Lrig3 constructs together with HA-Erk2 plasmid. Cells were treated with GDNF (50 ng/ml) as indicated. Total lysates were immunoprecipitated (IP) with anti-HA antibodies followed by immunoblot with anti-phospho Erk1/2 antibodies. The same blot was re-probed with anti-HA antibodies. Expression of Flag-Lrig3 in total cell lysates is also shown. (E) Bar graph showing quantification of Erk2 phosphorylation. Results are presented as fold change of Erk2/MAPK activation relative to control untreated samples (dashed line). Data are presented as mean±s.d. from three independent experiments. *P<0.01, two-tailed Student's t-test. (F) MN1 cell differentiation mediated by GDNF (100 ng/ml) and soluble GFRα1-Fc (300 ng/ml) is inhibited by Lrig3 overexpression. Photomicrographs show MN1 cells co-transfected with empty vector or Flag-Lrig3 plasmid together with a GFP expression vector. Scale bar: 20 µm. (G) Bar graph showing quantification of the percentage of GFP-positive MN1 cells bearing neurites longer than one cell body diameter after 72 h of treatment with GDNF in the presence of soluble GFRα1-Fc. The results are presented as mean±s.e.m. of n=3 independent experiments. P<0.01, one-way ANOVA followed by Student–Newman Keuls test.

inhibitors. To explore this possibility, we examined whether Lrig family members could be induced by GDNF ligands in DRG sensory neurons. Real-time PCR analysis revealed that *Lrig1* and *Lrig3*, but not *Lrig2*, mRNA were significantly induced in DRG primary cultures treated with GDNF and NRTN (Fig. 2E). Together, these findings indicate that Lrig1 and Lrig3 are widely co-expressed and co-developmentally upregulated in DRG. Furthermore, our results suggest possible overlapping functions of Lrig1 and Lrig3 in the control of Ret signaling and biology in nonpeptidergic DRG neurons.

Lrig1 and Lrig3 act redundantly to control axonal growth of DRG sensory neurons in response to GDNF ligands

Based on previous work indicating that GDNF ligands promote axonal elongation of embryonic and postnatal DRG sensory neurons (Paveliev et al., 2004; Yan et al., 2003), we decided to explore whether Lrig1 and Lrig3 could modulate axonal growth and complexity of DRG sensory neurons in response to GDNF and NRTN. To evaluate this, we cultured DRG sensory neurons isolated from wild-type, *Lrig1*-deficient or *Lrig3*-deficient mice. The cultures were maintained in the presence of the ligands and followed by staining with the neuronal marker βIII-tubulin. Because of the inhibitory role of Lrig1 and Lrig3 on Ret signaling, we expected to find potentiation of neurite outgrowth among the *Lrig1*- and *Lrig3*-deficient neurons. However, Lrig1- or Lrig3-deficient neurons showed axonal growth in response to GDNF ligands that was similar to that of the wild-type control neurons (Fig. 3A,B).

Previous evidence has demonstrated that Lrig family members can act both independently and redundantly during inner ear

Development (2021) 148, dev197020. doi:10.1242/dev.197020

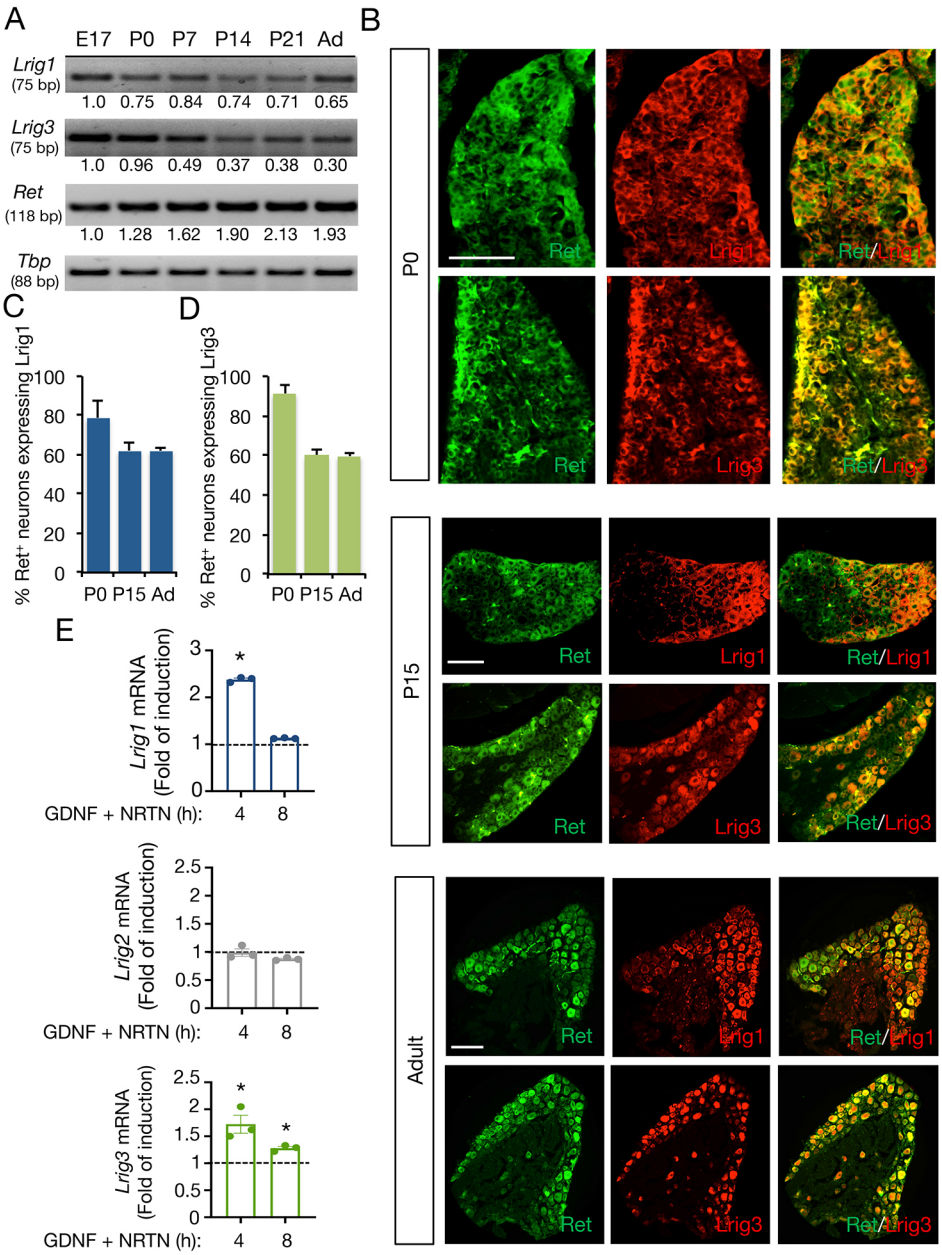

Fig. 2. Lrig1 and Lrig3 are expressed in Ret-positive DRG neurons and induced by GFLs in sensory primary neurons. (A) Semiquantitative analysis of the developmental expression of *Lrig1*, *Lrig3* and *Ret* mRNA by RT-PCR in DRG ganglia at E17, P0, P7, P14, P21 and adult (Ad) mice. Numbers are the average of three independent assays and indicate fold change of mRNA relative to E17. Expression at each age was normalized to that of the housekeeping gene *Tbp*. For each molecule, the PCR amplification product size is indicated in base pairs (bp). (B) Immunofluorescence staining showing co-expression of Ret/Lrig1 and Ret/Lrig3 in lumbar DRG sections from newborn (P0), P15 and adult mice. Scale bars: 100 µm. (C,D) Quantitative analysis of the percentage of Ret-positive neurons co-expressing either Lrig1 (C) or Lrig3 (D) in P0, P15 and adult (Ad) lumbar DRG sections. Bars show mean±s.e.m., n=8 sections from 3 mice. (E) Quantitative analysis of *Lrig1*, *Lrig2* and *Lrig3* mRNA expression by real-time PCR in rat DRG primary cultures treated with GDNF (30 ng/ml) and NRTN (30 ng/ml) for the indicated times (h). The levels of *Lrig* mRNAs were normalized using the expression of the house-keeping gene *Tbp*. Results are presented as fold change in stimulated cultures relative to control untreated samples (dashed line). Shown are mean±s.e.m., n=3 independent cultures. *P<0.01 versus control group (t=0 h) (one-way ANOVA followed by Dunnett's test).

development. In this structure, Lrig1 and Lrig3 expression overlaps prominently, and simultaneous removal of both genes disrupts inner ear morphogenesis (Del Rio et al., 2013). Given the significant induction of Lrig1 and Lrig3 by GDNF ligands in DRG neurons, we decided to explore further whether Lrig1 and Lrig3 might cooperate to control morphological differentiation of DRG neurons in response to GDNF and NRTN. Compared with wild-type cells, ablation of one copy of *Lrig1* from *Lrig3* mutant sensory neurons (*Lrig1HT/Lrig3KO*) significantly potentiated axonal growth and complexity in response to GDNF ligands (Fig. 3C-E). Then, we examined the phosphorylation status of the Ret downstream signaling effectors Erk1 and 2, which control axonal extension in sensory neurons in response to GFLs (Paratcha et al., 2001). In agreement with the outgrowth assays, *Lrig1* haploinsufficiency in *Lrig3*-deficient sensory neurons resulted in a significant increase of Erk1/2 activation in response to GDNF and NRTN (Fig. 3F,G).

Notably, these findings suggest that these two Lrig family members act redundantly to inhibit Ret downstream signaling and the morphological differentiation of DRG sensory neurons in response to GDNF family ligands.

Lrig1 and Lrig3 act redundantly to regulate epidermal innervation of nonpeptidergic GFRα1/2-positive fibers

Based on our results indicating that only DRG neurons obtained from *Lrig1HT/Lrig3KO* mice showed significant potentiation of axonal growth and complexity in response to GFLs (Fig. 3C-E), we decided to assess the cutaneous innervation of nociceptive fibers, a developmental process for which Ret signaling is required (Luo et al., 2007). We performed this analysis in wild-type, *Lrig3* knockout (*Lrig3KO*) and *LrigHT/Lrig3KO* mice. *Lrig1* knockout mice develop psoriasiform epidermal hyperplasia (Suzuki et al., 2002), which has been shown to increase nonpeptidergic intraepidermal fiber innervation (Sakai et al., 2017), and *Lrig1/Lrig3* double mutant mice die around birth (Del Rio et al., 2013), precluding analysis in these other mouse genetic backgrounds. To analyze epidermal innervation, free nerve endings in the glabrous hind paw skin were visualized using

Development (2021) 148, dev197020. doi:10.1242/dev.197020

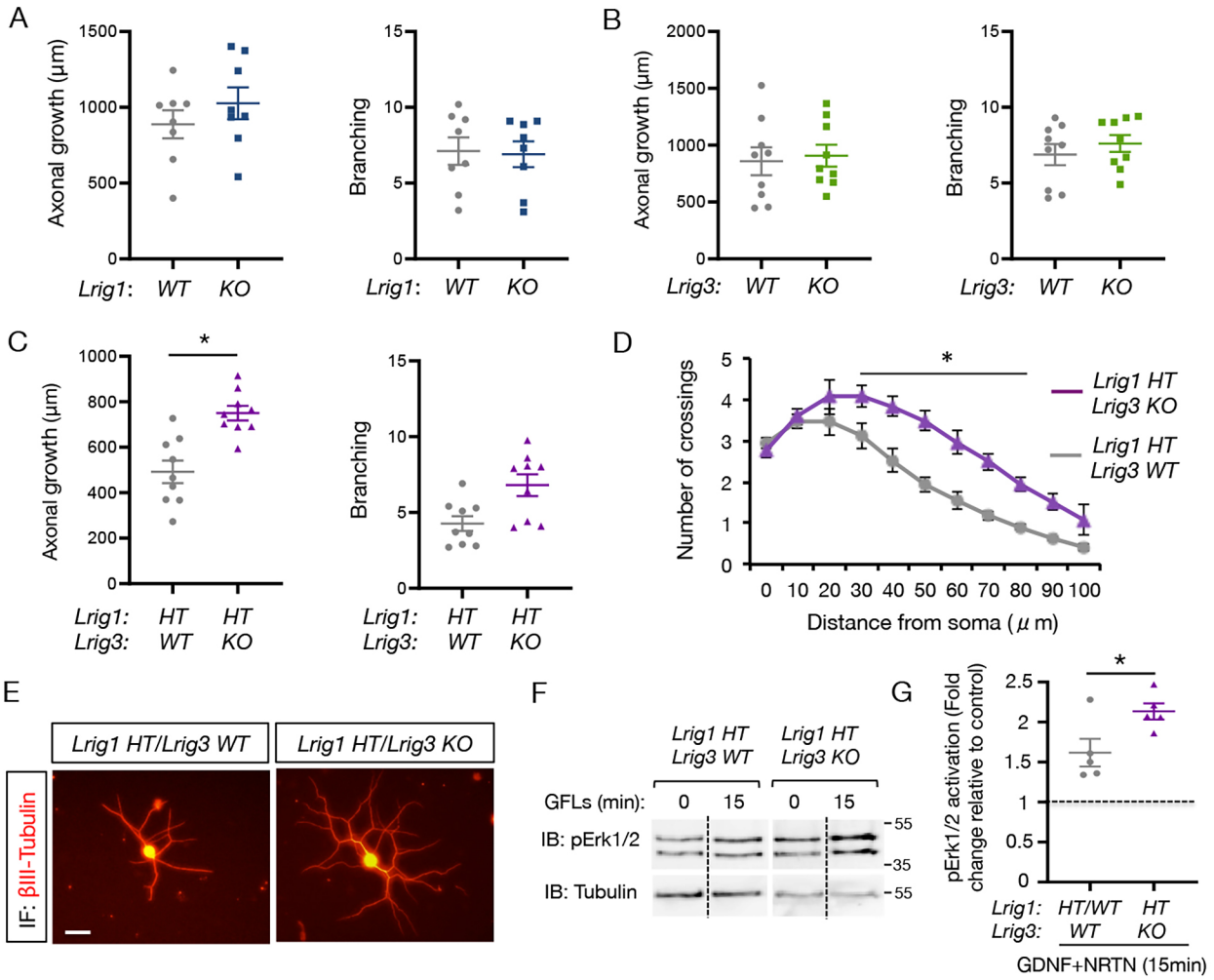

Fig. 3. Lrig1 and Lrig3 act redundantly to control GFL signaling and Ret-induced axonal growth of DRG sensory neurons. (A-C) Graphs showing axonal growth and branching of dissociated DRG primary neurons obtained from *Lrig1WT* versus *Lrig1KO* (A), *Lrig3WT* versus *Lrig3KO* (B) and *Lrig1 HT/Lrig3WT* versus *Lrig1HT/Lrig3KO* (C) P0 mice. Sensory neurons were treated for 24-36 h with GDNF (30 ng/ml) and NRTN (30 ng/ml), fixed and stained with the neuronal marker βIII-tubulin. Data are mean±s.e.m., *n*=3 mice from each genotype. Individual values represent average well determinations (30-60 neurons/mice). **P*<0.05, two tailed Student's *t*-test. (D) Sholl analysis of the axonal arbors of *Lrig1HT/Lrig3WT* versus *Lrig1HT/Lrig3KO* sensory neurons treated with GDNF and NRTN as described above. Graph shows the number of times that axons pass (crossings) across concentric circles localized at different distances from the cell bodies. The results are shown as mean±s.e.m., *n*=3 mice from each genotype (30 neurons/animal). **P*<0.05, two-way ANOVA followed by Bonferroni multiple comparisons test. (E) Representative images of βIII-tubulin-immunostained *Lrig1HT/Lrig3WT* and *Lrig1HT/Lrig3KO* DRG sensory neurons treated for 24 h with GDNF (30 ng/ml) and NRTN (30 ng/ml). IF, immunofluorescence. Scale bar: 25 µm. (F) Representative immunoblotting of Erk1/2 activation in cell extracts prepared from DRG primary cultures obtained from *Lrig1HT/Lrig3WT* and *Lrig1HT/Lrig3KO* treated for 15 min with 25 ng/ml of GDNF and NRTN (GFLs). Re-probing of the same blot with anti-βIII-tubulin is shown as a loading control. (G) Graph showing the quantification of Erk1/2 phosphorylation. Results are presented as fold change of Erk1/2/MAPK activation relative to control untreated samples (dashed line). Erk phosphorylation was normalized to the signal intensity of βIII-tubulin. Results are presented as mean±s.e.m. from *n*=5 *Lrig1HT/Lrig3WT and Lrig1WT/Lrig3WT* mice and *n*=5 *Lrig1HT/Lrig3KO* mice. **P*≤0.05, two-tailed Student's *t*-test.

antibodies against calcitonin gene-related peptide (CGRP) and the GFRα1/GFRα2 receptors for peptidergic and nonpeptidergic fiber assessment, respectively. Quantification of fibers showed that the epidermal density of CGRP-positive nerve fibers was unchanged between wild-type (*Lrig1WT/Lrig3WT*), *Lrig1WT/Lrig3KO* and *Lrig1HT/Lrig3KO* mice, whereas the density of GFRα1/2-positive nerve fibers in the epidermis increased in *Lrig1HT/Lrig3KO* animals compared with wild-type and *Lrig1WT/Lrig3KO* mice (Fig. 4A-C). There were ≈37% more GFRα1/2-positive fibers in the epidermis per unit length in *Lrig1HT/Lrig3KO* mice than in wild-type littermates, and no difference was detected between wild-type and *Lrig1WT/Lrig3KO* mice (Fig. 4C). This finding indicates that Lrig1 and Lrig3 act redundantly to ensure proper cutaneous innervation of nonpeptidergic axons expressing GFL receptors.

Role of Lrig1 and Lrig3 in control of the soma size of nonpeptidergic nociceptive neurons

Previous findings have established that Ret signaling is required for the acquisition of normal soma size but not survival of nonpeptidergic DRG nociceptors (Luo et al., 2007). Based on this evidence, we investigated the possibility of neuronal hypertrophy in *Lrig1HT/Lrig3KO* DRGs. In order to selectively identify nonpeptidergic nociceptive neurons, we performed immunofluorescence for Ret and peripherin, a neurofilament-associated protein expressed in nociceptive DRG neurons, followed by cell size analysis of double-positive neurons. The population of peripherin/Ret-positive neurons in P15 *Lrig1HT/Lrig3KO* mice showed a significant increase (≈25%) in mean soma area compared with control wild-type (*Lrig1WT/Lrig3WT*) mice.

Development (2021) 148, dev197020. doi:10.1242/dev.197020

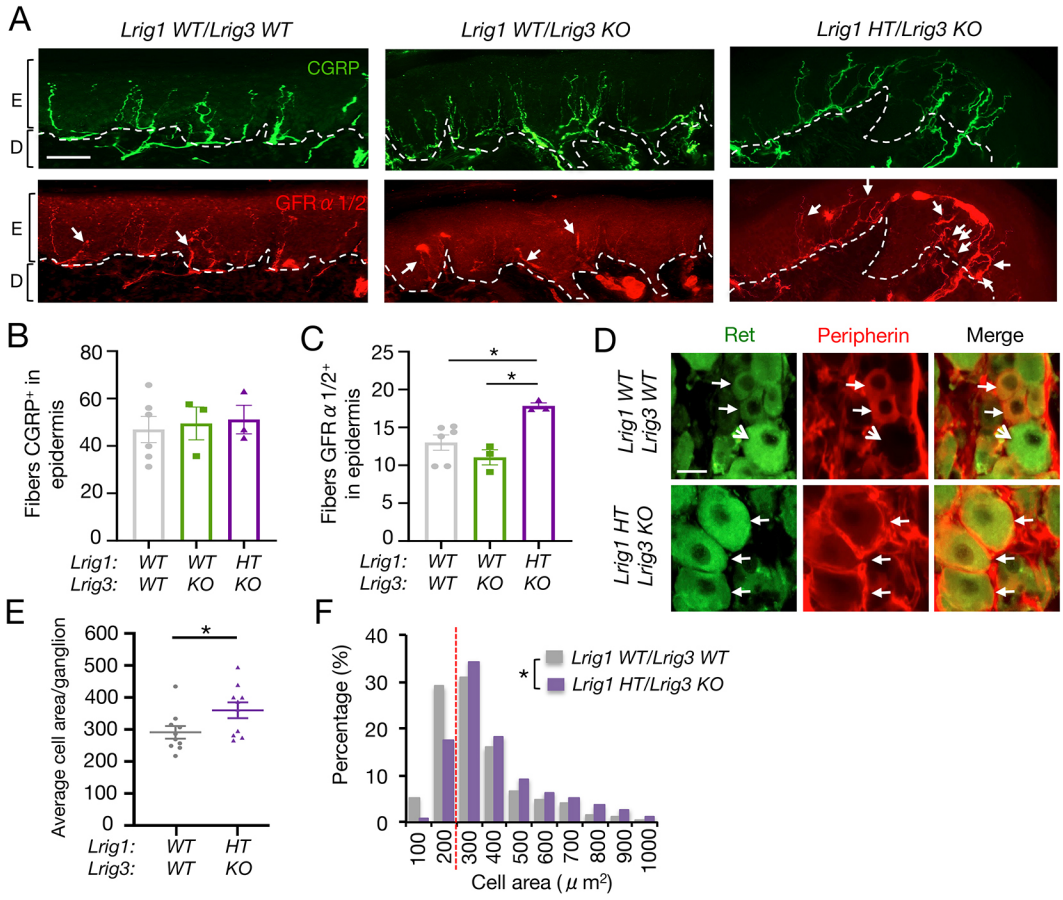

Fig. 4. Cooperation between Lrig1 and Lrig3 controls cutaneous innervation and soma size of nonpeptidergic nociceptive neurons. (A) Immunolabeling of glabrous footpad skin from wild-type, *Lrig1WT/Lrig3KO* and *Lrig1HT/Lrig3KO* mice stained for the peptidergic nociceptive marker CGRP and the GFL co-receptors GFRα1/GFRα2 (red), which label nonpeptidergic fibers. Dashed line delineates the boundary between epidermis and dermis. Arrows show GFRα1/GFRα2^{+} fibers in the epidermis. D, dermis; E, epidermis. Scale bar: 50 µm. (B,C) Bar graphs show the quantification of the number of CGRP-positive (B) and GFRα1/GFRα2-positive CGRP-negative (C) nerve fibers per unit length (1 mm) of epidermis obtained from wild-type, *Lrig1WT/Lrig3KO* and *Lrig1HT/Lrig3KO* mice. Data are expressed as mean±s.e.m., *n*=3 mice of each genotype (12 sections/mice). **P*<0.05, ANOVA followed by Bonferroni post-hoc test. (D) Ret (green) and peripherin (red) immunostaining in lumbar DRGs of wild-type (WT) and *Lrig1HT/Lrig3KO* mice at P15. Arrows show the hypertrophic soma of Ret/peripherin double-positive nonpeptidergic nociceptive neurons present in *Lrig1HT/Lrig3KO* DRGs. Arrowheads show the soma of a Ret-positive peripherin-negative neuron, representing mechanoreceptor neurons that were not included in the quantifications shown in E and F. (E) Graph showing the average neuronal area/ganglion±s.e.m. of *n*=10 ganglia from 2 mice of each genotype. **P*<0.05, two-tailed Student's *t*-test. (F) Cell size histogram displaying the percentage distribution of soma area of WT and *Lrig1HT/Lrig3KO* nonpeptidergic sensory neurons co-stained with Ret and peripherin. At least 495 neurons of lumbar DRGs from *n*=2 mice of each genotype were scored. Dashed red line indicates the soma size from which a significant rightward shift in the distribution of WT versus mutant neurons is observed. **P*<0.05, χ^2 test.

This hypertrophic effect is also reflected through a noticeable shift towards larger size in the population distribution of soma area of Lrig mutant neurons (Fig. 4D-F). We also assessed the nonpeptidergic nociceptive (peripherin^{+}/Ret^{+}) neuronal cell density in lumbar DRG sections as a measure of neuronal survival. No difference was observed in the nonpeptidergic nociceptive cells isolated from wild-type and *Lrig1HT/Lrig3KO* mice, indicating that this Lrig deficiency does not affect neuronal viability (Fig. S4).

Thus, this finding indicates that loss of one copy of *Lrig1* from *Lrig3* mutants compromises the acquisition of normal soma size of nonpeptidergic DRG nociceptors, without affecting the survival of these neurons. This finding is in agreement with a role of Lrig1 and Lrig3 as endogenous inhibitors of Ret activity.

Lrig1 and Lrig3 cooperate in the behavioral response to cold

Based on the increased epidermal innervation observed in *Lrig1HT/Lrig3KO* and the evidence indicating that alterations in nonpeptidergic innervation correlate with behavioral sensitivity to cold (Elitt et al., 2006; Wang et al., 2013), we decided to analyze the thermal responsiveness of *Lrig1HT/Lrig3KO* mice. We used the water tail-flick test in which a thermal stimulus was applied to the tail of the mouse and the time from onset of stimulation to rapid withdrawal of the tail from the water was recorded. The *Lrig1HT/Lrig3KO* mice exhibited significantly shorter withdrawal latencies in cold water (4°C) than wild-type or *Lrig3KO* mice. However, when the animals were stimulated with water at 48°C or 55°C, we did not observe differences between wild-type, *Lrig3KO* and *Lrig1HT/Lrig3KO* mice (Fig. 5A).

In agreement with this, a significant increase in the time of nociceptive response in the acetone test for cold, was observed in *Lrig1HT/Lrig3KO* compared with wild-type mice (Fig. 5B). No differences were detected in the latency time of paw withdrawal in the hotplate test at 48°C and 50°C (Fig. S5). Altogether, these results indicate that Lrig1 and Lrig3 contribute to cold-transduction mechanisms but not to heat sensitivity.

Development (2021) 148, dev197020. doi:10.1242/dev.197020

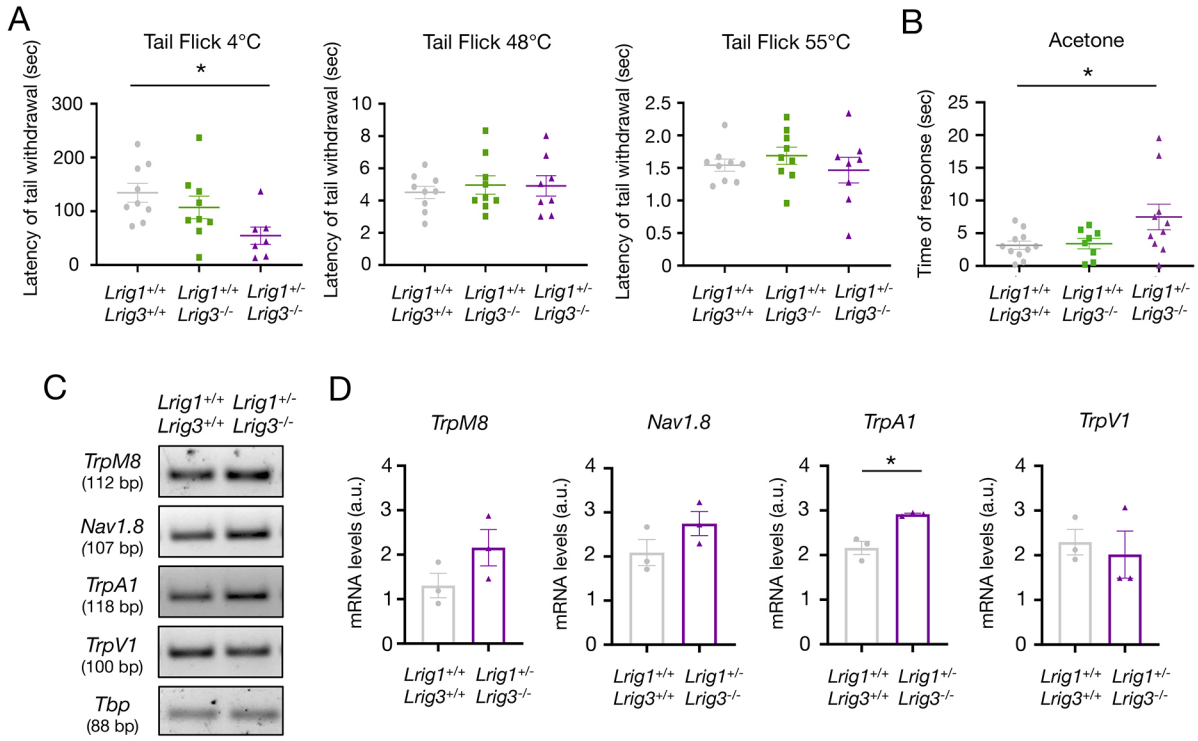

Fig. 5. *Lrig1HT/Lrig3KO* mice are hypersensitive to noxious cold. (A) Graphs showing individual values of the latency time (s) of tail withdrawal of *Lrig1WT/Lrig3WT* (*n*=9), *Lrig1WT/Lrig3KO* (*n*=9) and *Lrig1HT/Lrig3KO* (*n*=7-8) mice in the tail flick test at the indicated temperatures. Graphs show mean ±s.e.m. **P*<0.05, one-way ANOVA followed by Bonferroni post-hoc test. (B) Graph showing the results of the acetone evaporation test. Individual values correspond to the time (s) each animal spent in cold-evoked nocifensive behaviors in response to hind paw acetone application. *Lrig1WT/Lrig3WT* (*n*=11), *Lrig1WT/Lrig3KO* (*n*=8) and *Lrig1HT/Lrig3KO* (*n*=10). **P*<0.05, one-way ANOVA followed by Bonferroni post-hoc test. (C) Semiquantitative RT-PCR analysis of *TrpM8*, *Nav1.8*, *TrpA1* and *TrpV1* mRNA expression in lumbar DRGs obtained from 2-month-old wild-type and *Lrig1HT/Lrig3KO* mice. For each molecule, the PCR amplification product size is indicated in base pairs (bp). (D) Bar graphs showing *TrpM8*, *Nav1.8*, *TrpA1* and *TrpV1* mRNA levels expressed as arbitrary units (a.u.). The levels of mRNAs were normalized to the expression of the housekeeping gene *Tbp*. Data are expressed as mean±s.e.m. *n*=3 mice of each genotype, **P*<0.01, two-tailed Student's *t*-test.

The transduction of thermal information is mediated by temperature-sensitive ion channels mainly expressed in different sensory neurons (Buijs and McNaughton, 2020). To understand whether the cold sensitivity observed in *Lrig1HT/Lrig3KO* mice is accompanied by changes in transient receptor potential (TRP) ion channels, we evaluated by RT-PCR the mRNA expression of cold-sensing [*TrpM8*, *TrpA1*, *Nav1.8* (*Scn10a*)] and heat-sensing (*TrpV1*) channels in adult DRGs.

A significant increase in *TrpA1* mRNA expression was detected in adult DRG from *Lrig1HT/Lrig3KO* mice. Furthermore, a substantial, yet not significant, enhancement in the expression levels of *TrpM8* and *Nav1.8* was also observed (Fig. 5C,D). Interestingly, these results are in agreement with previous findings showing that TrpA1 and Nav1.8 contribute to cold nociception and thus correlate with the cold sensitivity observed in the tail-flick and acetone test (Kwan et al., 2006; Zimmermann et al., 2007).

Altogether, these results highlight the importance of genetic redundancy during neural development and show how dysregulation of endogenous neurotrophic factor inhibitors, such as Lrigs, contribute to developmental abnormalities that ultimately affect adult sensory behavior.

DISCUSSION

Transmembrane proteins containing extracellular LRR domains regulate neuronal connectivity functioning as modulators of axonal growth, dendrite morphogenesis and synapse formation. The members of this superfamily of proteins accomplish their functions by working as trans-synaptic cell adhesion molecules involved in synapse formation or functioning as cell-specific regulators of neurotrophic factor receptor trafficking and signaling.

Previously, we demonstrated that Lrig1 directly interacts with Ret and restricts GDNF-induced Ret signaling through inhibition of GDNF binding to Ret (Ledda et al., 2008). However, the contribution of other Lrig members for GDNF/Ret function has remained elusive. Here, we have shown that Lrig3 is able to associate with Ret and negatively regulate GFL/Ret signaling and neurite outgrowth, indicating that Lrig3 is an endogenous inhibitor of Ret. Our findings demonstrate that whereas single deletion of either *Lrig1* or *Lrig3* gene fails to enhance Ret-mediated neurite outgrowth above control values, *Lrig1* haploinsufficiency in *Lrig3* mutants significantly potentiates axonal growth of DRG sensory neurons in response to GDNF ligands.

The functional cooperation observed between Lrig1 and Lrig3 is in agreement with the selective induction of the expression of Lrig1 and Lrig3 detected in DRG sensory neurons treated with GDNF and NRTN (Fig. 2E). In line with this, we also observed that Lrig1 and Lrig3 act redundantly to ensure proper cutaneous sensory innervation of nonpeptidergic axons and behavioral sensitivity to cold (see Fig. 6), two events that are regulated by Ret signaling (Luo et al., 2007). Interestingly, the phenotypic change in footpad skin innervation detected in *Lrig1HT/Lrig3KO* mice resembles the high density of nonpeptidergic epidermal innervation observed in the skin of mice overexpressing different GFLs, such as GDNF, NRTN

Development (2021) 148, dev197020. doi:10.1242/dev.197020

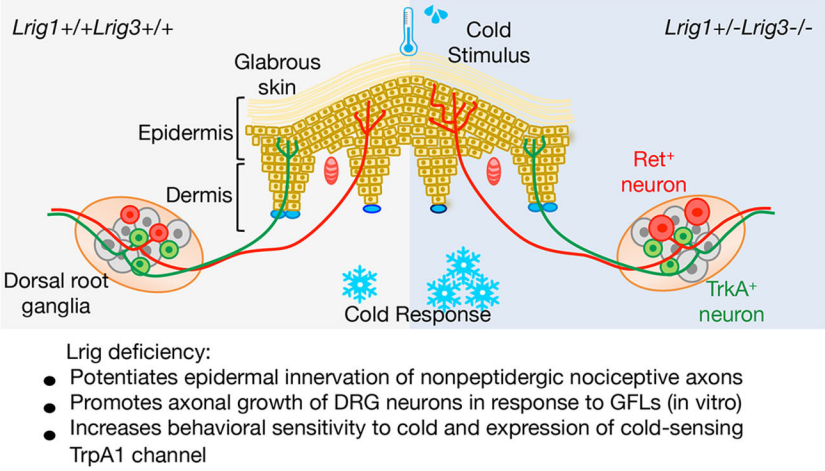

Fig. 6. Model summarizing the cooperative effects of Lrig1 and Lrig3 on DRG nociceptive neuronal connectivity and function. Haploinsufficiency of *Lrig1* in *Lrig3* knockout mice potentiates epidermal innervation of nonpeptidergic Ret-positive sensory axons (in red) and increases the behavioral response to cold stimulus.

and ARTN (Elitt et al., 2006; Wang et al., 2013; Zwick et al., 2002), and the deficient nonpeptidergic sensory innervation reported in GFRα2-deficient and *Ret* conditional knockout mice (Franck et al., 2011; Lindfors et al., 2006). This evidence additionally supports the role of Lrig1 and Lrig3 as endogenous inhibitors of the biological effects of GFRα/Ret in the innervation of DRG sensory axons.

The detection of noxious cold is crucial for mammals, which sense this information to avoid tissue damage and to maintain stable body temperature. We show here that *Lrig1HT/Lrig3KO* mice developed hypersensitivity to noxious cold and that this phenotype correlated with an increased expression of cold-sensitive ion channels that are expressed in Ret-positive nonpeptidergic sensory neurons, such as TrpA1 and Nav1.8 (Fig. 5A-C). Consistent with these findings, expression of TrpA1 and Nav1.8 are significantly reduced in *Ret*-conditional knockout mice (Franck et al., 2011; Luo et al., 2007), and ARTN overexpression in mouse skin enhances expression of TrpA1 in DRG neurons (Elitt et al., 2006). Taken together, this evidence additionally supports the role of Lrig1 and Lrig3 as endogenous inhibitors of the biological effects of GFRα/Ret in DRG neurons, contributing to thermal nociception.

Although the analysis of our data reveals that the vast majority of Lrig1- and Lrig3-positive neurons express Ret, we also observed that the expression of Lrig1 and Lrig3 exceeds the Ret-positive cell population, opening the possibility that Lrig1/Lrig3 might also have other physiological contributions on specific populations of Ret-negative sensory neurons.

Our *in vitro* and *in vivo* findings add valuable knowledge to a growing number of studies describing expression patterns and functional similarities between Lrig1 and Lrig3 in different tissues (Abraira et al., 2008; Del Rio et al., 2013; Homma et al., 2009). Furthermore, our study highlights genetic redundancy of Lrig1 and Lrig3 that serves to tightly control peripheral neuronal development, ultimately impacting the physiology of the adult animal. Although Lrig1 and Lrig3 cooperate during inner ear morphogenesis and nonpeptidergic skin innervation, each also has its own biological function. For instance, Lrig1 deficiency is sufficient to affect stem cell proliferation, hippocampal dendrite morphology and cochlear function *in vivo* (Alsina et al., 2016; Del Rio et al., 2013; Powell et al., 2012; Wong et al., 2012), whereas Lrig3 has been reported to regulate craniofacial development and lateral semicircular canal formation (Abraira et al., 2008) and neural crest formation in *Xenopus* embryos (Zhao et al., 2008).

Previous observations revealed that several LRR proteins, such as Lrig1, Linx, Lingo1 and AMIGO, may modulate development of specific populations of motor and sensory neurons by regulating neurotrophic factor receptor signaling during distinct stages of axonal growth, circuit formation and target-tissue innervation (Ledda et al., 2008; Ledda and Paratcha, 2016; Mandai et al., 2009). Whereas our previous and present characterization of Lrig1 and Lrig3 function show that they inhibit Ret function and biology, Linx promotes neurotrophin and GDNF signaling through physical association with Trk and Ret receptors, respectively (Mandai et al., 2009). Because of this, it has been proposed that LRR proteins have evolved to positively or negatively regulate RTK signaling, and therefore provide fine-tuned control over neurotrophic activity during development or in the adult nervous system. Hence, these cell type-specific regulators allow us to understand how a discrete number of neurotrophic factors can control the complexity of the neuronal connectivity.

GDNF ligands play crucial roles promoting survival and differentiation of midbrain dopaminergic and spinal cord motor neurons, two neuronal population involved in neurodegenerative disorders, such as Parkinson's disease and amyotrophic lateral sclerosis, respectively. Thus, understanding the endogenous mechanisms that control GDNF-induced Ret signaling could open new therapeutic opportunities for the treatment of these neurodegenerative disorders. Although the physiological relevance of Ret signaling inhibition by Lrig1 and Lrig3 in those neuronal populations requires additional investigation, the data presented here suggest that targeting Lrig1 and/or Lrig3 in dopaminergic and motor neurons could enhance therapeutic activities of GDNF for nerve injury and neurodegeneration.

In peripheral sensory neurons, GDNF or NRTN treatment can improve cutaneous innervation deficits caused by diabetes (Christianson et al., 2003a,b). Based on our findings, it is logical to hypothesize that dysregulation of Lrig1 and/or Lrig3 in these neuronal populations may contribute to the pathogenesis of neurodegenerative diseases and to defects of sensory innervation. Therefore, understanding the mechanisms that endogenously control GDNF ligand-induced Ret signaling appears to be a potential target of therapy for neurodegenerative disorders and sensory regeneration.

MATERIALS AND METHODS

Recombinant proteins, reagents and cell lines

HEK-293T (from American type culture collection, ATCC) cells were grown in Dulbecco's modified Eagle's medium (DMEM) supplemented with 10% fetal bovine serum (FBS, Invitrogen). MN1 is an immortalized mouse-derived motor neuron cell line responsive to GDNF that was cultured

Development (2021) 148, dev197020. doi:10.1242/dev.197020

in DMEM supplemented with 7.5% FBS, HEPES (10 mM, Invitrogen) as previously described (Alsina et al., 2016; Ledda et al., 2008). GDNF and NRTN were purchased from R&D Systems.

RT-PCR and qPCR

The expression of *Lrig1*, *Lrig2*, *Lrig3*, *Ret* and TATA box-binding protein (*Tbp*) mRNAs were analyzed by semiquantitative PCR from total RNA isolated from mouse DRG obtained at different embryonic (E) and postnatal (P) stages. Expression of ion channel mRNAs (*Nav1.8*, *TrpA1*, *TrpM8* and *TrpV1*) were analyzed by semiquantitative PCR from total RNA isolated from lumbar DRGs obtained from 2-month-old wild-type and *Lrig1HT/Lrig3KO* mice. Rat primary DRG cultures were used to analyze by real-time qPCR the induction of Lrig members in response to GDNF and NRTN. In all cases, RNA was isolated using RNA-easy columns (Qiagen). cDNA was synthesized using multiscribe reverse transcriptase and random hexamers (Applied Biosystems). The cDNA was amplified using the following primer sets: *Tbp*: forward 5′-GGGGAGCTGTGATGTGAAGT-3′, reverse 5′-CCAGGAAATAATTCTGGCTCA-3′; rat *Lrig1*: forward 5′-CTGCGTGTAAGGGAACTCAAC-3′, reverse 5′-GATAGACCATCA-AACGCTCCA-3′; mouse *Lrig1*: forward 5′-TCTGCAGGAAGTGTA-CCTCAACAG-3′; reverse 5′-GAGAGACAACTCCTATGGAAGCAGT-3′; rat *Lrig2*: forward 5′-ACGACACAGCAGACCACAAC-3′, reverse 5′-CAGAGTAGCATTGGGCATGA-3′; rat and mouse *Lrig3*: forward 5′-GGCTCCGACGTGAGTTTTAC-3′, reverse 5′-GTCTTTCTTCCAAG-CGAACG-3′; mouse *Ret*: forward 5′-TGAAGAAAAGCAAGGGCCGG-3′, reverse 5′-ACAATCTCCCAGAGCAGCAC-3′; mouse *Nav1.8*: forward 5′-CATGAAGAAGCTGGGCTCCA-3′, reverse 5′-TGATGTCAAATGC-TTGCCTGG-3′; mouse *TrpA1*: forward 5′-ATGCAAGAAACACGAC-AAGA-3′, reverse 5′-TGAGCTCATGCTGCTTTTCC-3′; mouse *TrpM8*: forward 5′-AAGAAGTGTTTCAAATGCTG-3′, reverse 5′-AATTCTC-CTTCATGACACCC-3′; mouse *TrpV1*: forward 5′-GACGGCAAGGAT-GACTTCCG-3′, reverse 5′-AGTTGCCTGGGTCCTCGTT-3′.

Real-time PCR was performed using the SYBR Green qPCR SuperMix (Invitrogen) in an ABI7500 Sequence Detection System (Applied Biosystems), according to the manufacturer's instructions. For semiquantitative PCR, gel bands were quantified using Gel-Pro Analyzer software.

Mouse strains

The *Lrig1* mutant mice have been described in detail by Alsina et al. (2016) and Mao et al. (2018), and *Lrig3* null mice have been described by Hellstrom et al. (2016). All mouse strains were maintained in heterozygosis and the tested mice were littermate progeny of matings between heterozygous Lrig KO mice. Animal experiments were in accordance with the institutional animal care and ethics committee of the School of Medicine (CICUAL-UBA). Ethical permit number: 902/2016.

Cell transfection and constructs

MN1 and HEK-293T cells were transfected with polyethylenimine (PEI; Polysciences). For biochemical assays, cells were transfected either with Flag-tagged Lrig1 or Flag-tagged Lrig3 constructs together with Ret or HA-tagged Erk2 plasmids.

Plasmid cDNA encoding full-length Flag-tagged Lrig1 has been described previously (Ledda et al., 2008). The plasmid encoding Flag-tagged-Lrig3 was kindly provided by Lisa Goodrich (Harvard Medical School, USA) (Abraira et al., 2010). The plasmid encoding GFP was obtained from Clontech.

Sensory neuron cultures

Primary DRG neuronal cultures were prepared from E20 Wistar rats or P0 newborn mice. Briefly, the lumbar ganglia were dissociated with collagenase (0.1% w/v, Sigma-Aldrich), trypsin (0.1% w/v, Invitrogen) and DNaseI (10 µg/ml, Invitrogen), and then seeded onto plates coated with poly-ornithine (0.5 mg/ml, Sigma-Aldrich) and laminin (10 µg/ml, Sigma-Aldrich). The neurons were maintained in DMEM/F12 medium supplemented with 60 µg/ml penicillin, 100 µg/ml streptomycin, 2 mM glutamine (Invitrogen), 1 mg/ml bovine serum albumin (BSA; Sigma-Aldrich), and supplemented with GFLs (GDNF plus NRTN) at 30 ng/ml each.

Total cell lysates, immunoprecipitation and western blotting

Cells were lysed at 4°C in TNE buffer (50 mM Tris pH 7.5, 150 mM NaCl and 2 mM EDTA) supplemented with 0.5% Triton X-100, 1% β-octylglucoside plus phosphatase inhibitors (50 mM NaF, 2 mM Na_3VO_4) and complete EDTA-free protease inhibitors (Roche). Protein lysates were clarified by centrifugation (10,000 ***g*** for 10 min) and analyzed by immunoprecipitation and western blotting using previously described methodologies (Alsina et al., 2016). The antibodies were obtained from various sources as follows: anti-phosphotyrosine (p-Tyr, clone PY99, sc-7020; 1/1000) and anti-Ret (c-20, sc-1290 and t-20, sc-1291; 1/500 of each) were from Santa Cruz Biotechnology; anti-p-Erk1/2 (Thr-202/Tyr-204, 9101; 1/2000) and anti-p-Akt (Ser 473, 9271; 1/1000) were from Cell Signaling; anti-HA (11666606001, clone 12CA5; 1/1000) was from Roche; and anti-Flag M2 antibody (F1804; 1/2500) was from Sigma-Aldrich.

All blots were scanned in a Storm 845 PhosphorImager (GE Healthcare Life Sciences), and quantifications were performed with ImageQuant software (GE Healthcare Life Sciences).

Immunofluorescence and microscopy

For colocalization and soma size quantification assays, newborn or P15 mice of selected genotypes were euthanized, perfused transcardially with 4% paraformaldehyde (PFA) in PBS under deep anesthesia. The lumbar section of the spinal cord and dorsal root ganglia were dissected and postfixed overnight. Serial cryosections (20 µm) were made using a Leica CM1850 cryostat and processed for immunofluorescence as follows. Cryosections were permeabilized with 0.1% Triton X-100 in PBS for 30 min, washed three times with PBS 10 min each, blocked with 10% donkey serum (Jackson ImmunoResearch) and 0.01% Triton X-100 in PBS for 60 min and then incubated overnight with a solution containing 3% BSA (Sigma-Aldrich) in PBS and primary antibodies against Ret (AF482, R&D Systems; 1:200) and anti-peripherin (MAB1527, clone 8G2, Chemicon; 1:400), a neurofilament protein which is expressed selectively in both peptidergic and nonpeptidergic cutaneous neurons. Sections were then washed with PBS five times for 20 min each and then incubated with the following secondary antibodies from Jackson ImmunoResearch: Cy2-donkey anti-rabbit IgG (H+L) (711-225-152; 1/300); Cy3-donkey anti-rabbit IgG (H+L) (711-165-152; 1/300); Cy2-donkey anti-goat IgG (H+L) (705-225-147; 1/300); Cy3-donkey anti-goat IgG (H+L) (705-165-147; 1/300) and Cy3-donkey anti-mouse IgG (H+L) (715-165-150; 1/300).

For soma size quantification, images were obtained using an Olympus IX83 DSU 20× objective. Images were acquired using the same settings with no saturation and no bleedthrough and minimized noise at a resolution of 2048×2048 pixels (16 bit). Each image corresponds to a merged stack 10 µm thick, composed of optical sections of 1 µm each. For soma size analysis, double-positive Ret/peripherin cells were outlined and measured using ImageJ FIJI software. Only cells with a clear nucleus were scored.

For Lrig/Ret colocalization, images were obtained using an Olympus confocal FV1000 microscope, employing a 40×1.30 NA immersion oil objective with the sequential acquisition setting. Images were acquired with a resolution of 800×800 (12 bit). A *z*-series projection of each DRG was made. Each image corresponds to a merged stack of 14 µm thick composed of optical sections of 2 µm each.

For immunostaining of hind paw glabrous skin sensory innervation, we followed the protocol described by Zylka et al. (2005). Briefly, adult mice of selected genotypes were euthanized by perfusion with Zamboni's solution under deep anesthesia. Glaborous hind paw skin was dissected and postfixed overnight. Epidermal innervation was visualized in 50-µm-thick serial cryosections using antibodies against the peptidergic nociceptive marker CGRP or using a mixture of antibodies against GFRα1 and GFRα2 receptors, which label nonpeptidergic nociceptive DRG sensory neurons (Sakai et al., 2017). Images were obtained using an Olympus IX83 DSU 20× objective at a resolution of 2048×2048 pixels (16 bits). Each image corresponds to a 20-µm-thick merged stack composed of optical sections of 1 µm each. The number of fibers on segments of 1 mm of skin were evaluated using ImageJ software.

The following antibodies were used for immunofluorescence assays: goat polyclonal anti-Ret extracellular domain (AF482, R&D Systems; 1/200), goat polyclonal anti-GFRα1 (AF560, R&D Systems; 1/200); goat

Development (2021) 148, dev197020. doi:10.1242/dev.197020

polyclonal anti-GFRα2 (AF429, R&D Systems; 1/200); rabbit anti anti-CGRP (PC205L, Sigma-Aldrich; 1/1000), anti-peripherin (MAB1527, clone 8G2, Chemicon; 1:400); rabbit polyclonal anti-Lrig1 extracellular domain (gift from Dr Satoshi Itami, University of Osaka, Osaka, Japan; 1/1000; Alsina et al., 2016; Suzuki et al., 2002) and rabbit polyclonal anti-Lrig3 (mLrig3-207; 1/200; Hellstrom et al., 2016). The specificity of mLirg3-207 antibody was validated using knockout cell extract and tissue for immunoblotting and immunofluorescence, respectively (Fig. S3). The specificity of anti-Lrig1 (Alsina et al., 2016), anti-GFRα1 (Irala et al., 2016; Sergaki et al., 2017), anti-GFRα2 (Lindfors et al., 2006) and anti-Ret (Park and Bolton, 2017) antibodies have been previously validated using knockout tissue. Secondary antibodies were from Jackson ImmunoResearch: Cy2-donkey anti-rabbit IgG (H+L) (711-225-152; 1/300); Cy3-donkey anti-rabbit IgG (H+L) (711-165-152; 1/300); Cy2-donkey anti-goat IgG (H+L) (705-225-147; 1/300); Cy3-donkey anti-goat IgG (H+L) (705-165-147; 1/300) and Cy3-donkey anti-mouse IgG (H+L) (715-165-150; 1/300).

Neurite outgrowth assays

Neurite outgrowth was performed in MN1 cells co-transfected with either control or Flag-Lrig3 vectors and GFP. The next day, the cells were plated on 24-well plates coated with rat-tail collagen (Millipore) and cultured in 1% FBS-containing DMEM supplemented with GDNF (100 ng/ml) plus soluble GFRα1-Fc (300 ng/ml) as previously described (Paratcha et al., 2001). After 72 h, the cells were fixed with 4% PFA. The number of MN1 cells bearing neurites longer than one cell body was quantified relative to the total number of GFP-positive cells counted in at least ten random fields of three different wells in each experiment. MN1 cell differentiation was evaluated in three independent experiments. Images were obtained using an Olympus IX-81 inverted microscope.

Primary cultures of DRG neurons were prepared as previously described (see above). Neurons were cultured in the presence of the apoptotic inhibitor Z-VAD-FMK (50 nM; Sigma-Aldrich) and GFLs (30 ng/ml; R&D Systems) for 24-36 h. Then, cells were fixed with 4% PFA and stained with anti-βIII-tubulin to identify neurites (mouse anti-βIII Tubulin, G7121, clone 5G8, Promega; 1/5000). Neuronal survival was assessed using the nuclear stain 4′,6-diamidino-2-phenylindole dihydrochloride (DAPI; Sigma-Aldrich). Neurons containing fragmented or condensed nuclear staining were scored as apoptotic cells and not computed in the differentiation assays. In the absence of the apoptotic inhibitor Z-VAD-FMK, no evident effect on cell viability was observed in neurons obtained from the different genetic backgrounds. Images were obtained using an Olympus IX-81 inverted microscope. Quantification of neurite length was performed using National Institutes of Health ImageJ software. Axonal complexity was analyzed using the Sholl plug-in of NeuronJ.

Behavioral assays

Behavior testing was performed using male mice of 8-10 weeks of age. Behavioral tests were conducted blind to the genotypes of the mice. Prior to testing, mice were acclimated to the environment 1 h daily for 3 days before the day of testing.

For the tail-flick test, mice were gently restrained and the distal half of the tail was inserted into a water bath at different temperatures: 4°C, 48°C and 55°C. The water bath temperatures were controlled either thermostatically (48°C and 55°C) or by a digital thermometer (4°C; bath surrounded with ice). The latency to withdraw the tail was recorded with a digital camera using Logitech Webcam Software.

For the acetone test, one drop of acetone was applied to the plantar surface of the hind paw to cause evaporative cooling. Mice were placed on a metal surface surrounded by a plastic cylinder where they were observed and recorded for 5 min. Time spent eliciting spontaneous nociceptive behaviors (shaking, flinching, licking or biting the paw) was measured. Both paws were tested with a 15 min interval between each one.

For the hot plate assay, animals were placed in a hot plate device set at 48°C or 50°C surrounded by a plastic cylinder where they were observed and recorded. Mice were tested once for each temperature with a 60 min interval between them. Latency time until first pain behavior elicited (shaking, flinching or licking any paw) was measured.

Statistical analysis

Data are reported as mean±s.e.m. or s.d. as indicated, and significance was accepted at $P<0.05$. The number of independent experiments or the number of mice used in each experimental condition are described in figure legends. No statistical method was used to predetermine sample sizes, but our sample sizes are similar to those generally used in the field. The selection of the mice was unbiased in terms of size and weight. For animal studies, the handling of the data was performed blind. Statistical analyses were performed in GraphPad Prism 8.0. The normal distribution of the data was evaluated with the Shapiro–Wilk test or the Kolmogorov–Smirnov test. In each case, two-tailed Student's *t*-test or one-way ANOVA analysis followed by a respective post-hoc test are indicated in figure legends. χ^2 test was used to compare distribution of the percentage of cell areas.

Acknowledgements

We thank Dr Lisa V Goodrich for the Flag-Lrig3 construct, Dr Satoshi Itami for the anti-Lrig1 antibody, Andrea Pecile and Manuel Ponce for animal care, Lic. Nerina Villalba for technical assistance, Dr Jorge Aquino and Dr Pablo Brumovsky for experimental advice, and UBATEC for research grant administration.

Competing interests

The authors declare no competing or financial interests.

Author contributions

Conceptualization: A.P.D.V., F.C.A., F.F.R., H.H., F.L., G.P.; Methodology: A.P.D.V., F.C.A., F.F.R.; Formal analysis: A.P.D.V., F.C.A., F.F.R., F.L., G.P.; Investigation: A.P.D.V., F.C.A., F.F.R.; Resources: H.H.; Writing - original draft: G.P.; Writing - review & editing: G.P.; Supervision: F.L., G.P.; Funding acquisition: F.L., G.P.

Funding

This work was supported by the Argentine Agency for Promotion of Science and Technology (Agencia Nacional de Promoción Científica y Tecnológica, ANPCyT; PICT2015-3814, PICT2016-1512, PICT2017-4513, PICT2017-4597, PICT2019-1472). G.P. and F.L. were supported by an Independent Research Career Position from the Argentine Medical Research Council (Consejo Nacional de Investigaciones Científicas y Técnicas, CONICET). A.P.D.V., F.C.A. and F.F.R. were supported by fellowships from CONICET and ANPCyT.

References

Abraira, V. E., Del Rio, T., Tucker, A. F., Slonimsky, J., Keirnes, H. L. and Goodrich, L. V. (2008). Cross-repressive interactions between Lrig3 and netrin 1 shape the architecture of the inner ear. *Development* **135**, 4091-4099. doi:10.1242/dev.029330

Abraira, V. E., Satoh, T., Fekete, D. M. and Goodrich, L. V. (2010). Vertebrate Lrig3-ErbB interactions occur in vitro but are unlikely to play a role in Lrig3-dependent inner ear morphogenesis. *PLoS ONE* **5**, e8981. doi:10.1371/journal.pone.0008981

Airaksinen, M. S. and Saarma, M. (2002). The GDNF family: signalling, biological functions and therapeutic value. *Nat. Rev. Neurosci.* **3**, 383-394. doi:10.1038/nrn812

Airaksinen, M. S., Titievsky, A. and Saarma, M. (1999). GDNF family neurotrophic factor signaling: four masters, one servant? *Mol. Cell. Neurosci.* **13**, 313-325. doi:10.1006/mcne.1999.0754

Alsina, F. C., Hita, F. J., Fontanet, P. A., Irala, D., Hedman, H., Ledda, F. and Paratcha, G. (2016). Lrig1 is a cell-intrinsic modulator of hippocampal dendrite complexity and BDNF signaling. *EMBO Rep.* **17**, 601-616. doi:10.15252/embr.201541218

Alsina, F. C., Ledda, F. and Paratcha, G. (2012). New insights into the control of neurotrophic growth factor receptor signaling: implications for nervous system development and repair. *J. Neurochem.* **123**, 652-661. doi:10.1111/jnc.12021

Buijs, T. J. and McNaughton, P. A. (2020). The role of cold-sensitive ion channels in peripheral thermosensation. *Front. Cell Neurosci.* **14**, 262. doi:10.3389/fncel.2020.00262

Christianson, J. A., Riekhof, J. T. and Wright, D. E. (2003a). Restorative effects of neurotrophin treatment on diabetes-induced cutaneous axon loss in mice. *Exp. Neurol.* **179**, 188-199.

Christianson, J. A., Ryals, J. M., McCarson, K. E. and Wright, D. E. (2003b). Beneficial actions of neurotrophin treatment on diabetes-induced hypoalgesia in mice. *J. Pain* **4**, 493-504.

Del Rio, T., Nishitani, A. M., Yu, W. M. and Goodrich, L. V. (2013). In vivo analysis of Lrig genes reveals redundant and independent functions in the inner ear. *PLoS Genet.* **9**, e1003824. doi:10.1371/journal.pgen.1003824

Dolan, J., Walshe, K., Alsbury, S., Hokamp, K., O'Keeffe, S., Okafuji, T., Miller, S. F., Tear, G. and Mitchell, K. J. (2007). The extracellular leucine-rich repeat

superfamily; a comparative survey and analysis of evolutionary relationships and expression patterns. *BMC Genomics* **8**, 320. doi:10.1186/1471-2164-8-320

Durbec, P., Marcos-Gutierrez, C. V., Kilkenny, C., Grigoriou, M., Wartiowaara, K., Suvanto, P., Smith, D., Ponder, B., Costantini, F., Saarma, M. et al. (1996). GDNF signalling through the Ret receptor tyrosine kinase. *Nature* **381**, 789-793. doi:10.1038/381789a0

Elitt, C. M., McIlwrath, S. L., Lawson, J. J., Malin, S. A., Molliver, D. C., Cornuet, P. K., Koerber, H. R., Davis, B. M. and Albers, K. M. (2006). Artemin overexpression in skin enhances expression of TRPV1 and TRPA1 in cutaneous sensory neurons and leads to behavioral sensitivity to heat and cold. *J. Neurosci.* **26**, 8578-8587.

Franck, M. C., Stenqvist, A., Li, L., Hao, J., Usoskin, D., Xu, X., Wiesenfeld-Hallin, Z. and Ernfors, P. (2011). Essential role of Ret for defining non-peptidergic nociceptor phenotypes and functions in the adult mouse. *Eur. J. Neurosci.* **33**, 1385-1400. doi:10.1111/j.1460-9568.2011.07634.x

Fundin, B. T., Mikaels, A., Westphal, H. and Ernfors, P. (1999). A rapid and dynamic regulation of GDNF-family ligands and receptors correlate with the developmental dependency of cutaneous sensory innervation. *Development* **126**, 2597-2610. doi:10.1242/dev.126.12.2597

Guo, D., Holmlund, C., Henriksson, R. and Hedman, H. (2004). The Lrig gene family has three vertebrate paralogs widely expressed in human and mouse tissues and a homolog in Ascidiacea. *Genomics* **84**, 157-165. doi:10.1016/j.ygeno.2004.01.013

Guo, D., Yang, H., Guo, Y., Xiao, Q., Mao, F., Tan, Y., Wan, X., Wang, B. and Lei, T. (2015). LRIG3 modulates proliferation, apoptosis and invasion of glioblastoma cells as a potent tumor suppressor. *J. Neurol. Sci.* **350**, 61-68. doi:10.1016/j.jns.2015.02.015

Gur, G., Rubin, C., Katz, M., Amit, I., Citri, A., Nilsson, J., Amariglio, N., Henriksson, R., Rechavi, G., Hedman, H. et al. (2004). LRIG1 restricts growth factor signaling by enhancing receptor ubiquitylation and degradation. *EMBO J.* **23**, 3270-3281. doi:10.1038/sj.emboj.7600342

Hellstrom, M., Ericsson, M., Johansson, B., Faraz, M., Anderson, F., Henriksson, R., Nilsson, S. K. and Hedman, H. (2016). Cardiac hypertrophy and decreased high-density lipoprotein cholesterol in Lrig3-deficient mice. *Am. J. Physiol. Regul. Integr. Comp. Physiol.* **310**, R1045-R1052. doi:10.1152/ajpregu.00309.2015

Henderson, C. E., Phillips, H. S., Pollock, R. A., Davies, A. M., Lemeulle, C., Armanini, M., Simmons, L., Moffet, B., Vandlen, R. A., Simpson, L. C. et al. (1994). GDNF: a potent survival factor for motoneurons present in peripheral nerve and muscle. *Science* **266**, 1062-1064. doi:10.1126/science.7973664

Homma, S., Shimada, T., Hikake, T. and Yaginuma, H. (2009). Expression pattern of LRR and Ig domain-containing protein (LRRIG protein) in the early mouse embryo. *Gene Expr. Patterns* **9**, 1-26. doi:10.1016/j.gep.2008.09.004

Irala, D., Bonafina, A., Fontanet, P. A., Alsina, F. C., Paratcha, G. and Ledda, F. (2016). The GDNF-GFRalpha1 complex promotes the development of hippocampal dendritic arbors and spines via NCAM. *Development* **143**, 4224-4235.

Jing, S., Wen, D., Yu, Y., Holst, P. L., Luo, Y., Fang, M., Tamir, R., Antonio, L., Hu, Z., Cupples, R. et al. (1996). GDNF-induced activation of the ret protein tyrosine kinase is mediated by GDNFR-alpha, a novel receptor for GDNF. *Cell* **85**, 1113-1124. doi:10.1016/S0092-8674(00)81311-2

Kramer, E. R., Knott, L., Su, F., Dessaud, E., Krull, C. E., Helmbacher, F. and Klein, R. (2006). Cooperation between GDNF/Ret and ephrinA/EphA4 signals for motor-axon pathway selection in the limb. *Neuron* **50**, 35-47.

Kwan, K. Y., Allchorne, A. J., Vollrath, M. A., Christensen, A. P., Zhang, D.-S., Woolf, C. J. and Corey, D. P. (2006). TRPA1 contributes to cold, mechanical, and chemical nociception but is not essentil for hair-cell transduction. *Neuron* **50**, 277-289. doi:10.1016/j.neuron.2006.03.042

Laederich, M. B., Funes-Duran, M., Yen, L., Ingalla, E., Wu, X., Carraway, K. L., III and Sweeney, C. (2004). The leucine-rich repeat protein LRIG1 is a negative regulator of ErbB family receptor tyrosine kinases. *J. Biol. Chem.* **279**, 47050-47056. doi:10.1074/jbc.M409703200

Lallemend, F. and Ernfors, P. (2012). Molecular interactions underlying the specification of sensory neurons. *Trends Neurosci.* **35**, 373-381. doi:10.1016/j.tins.2012.03.006

Ledda, F., Bieraugel, O., Fard, S. S., Vilar, M. and Paratcha, G. (2008). Lrig1 is an endogenous inhibitor of Ret receptor tyrosine kinase activation, downstream signaling, and biological responses to GDNF. *J. Neurosci.* **28**, 39-49. doi:10.1523/JNEUROSCI.2196-07.2008

Ledda, F. and Paratcha, G. (2016). Assembly of neuronal connectivity by neurotrophic factors and leucine-rich repeat proteins. *Front. Cell. Neurosci.* **10**, 199. doi:10.3389/fncel.2016.00199

Li, L., Wu, W., Lin, L. F., Lei, M., Oppenheim, R. W. and Houenou, L. J. (1995). Rescue of adult mouse motoneurons from injury-induced cell death by glial cell line-derived neurotrophic factor. *Proc. Natl. Acad. Sci. USA* **92**, 9771-9775.

Lindfors, P. H., Voikar, V., Rossi, J. and Airaksinen, M. S. (2006). Deficient nonpeptidergic epidermis innervation and reduced inflammatory pain in glial cell line-derived neurotrophic factor family receptor alpha2 knock-out mice. *J. Neurosci.* **26**, 1953-1960. doi:10.1523/JNEUROSCI.4065-05.2006

Luo, W., Wickramasinghe, S. R., Savitt, J. M., Griffin, J. W., Dawson, T. M. and Ginty, D. D. (2007). A hierarchical NGF signaling cascade controls Ret-dependent and Ret-independent events during development of nonpeptidergic DRG neurons. *Neuron* **54**, 739-754.

Mandai, K., Guo, T., St Hillaire, C., Meabon, J. S., Kanning, K. C., Bothwell, M. and Ginty, D. D. (2009). LIG family receptor tyrosine kinase-associated proteins modulate growth factor signals during neural development. *Neuron* **63**, 614-627. doi:10.1016/j.neuron.2009.07.031

Mao, F., Holmlund, C., Faraz, M., Wang, W., Bergenheim, T., Kvarnbrink, S., Johansson, M., Henriksson, R. and Hedman, H. (2018). Lrig1 is a haploinsufficient tumor suppressor gene in malignant glioma. *Oncogenesis* **7**, 13. doi:10.1038/s41389-017-0012-8

Marmigere, F. and Ernfors, P. (2007). Specification and connectivity of neuronal subtypes in the sensory lineage. *Nat. Rev.* **8**, 114-127. doi:10.1038/nrn2057

Meabon, J. S., De Laat, R., Ieguchi, K., Wiley, J. C., Hudson, M. P. and Bothwell, M. (2015). LINGO-1 protein interacts with the p75 neurotrophin receptor in intracellular membrane compartments. *J. Biol. Chem.* **290**, 9511-9520. doi:10.1074/jbc.M114.608018

Molliver, D. C., Wright, D. E., Leitner, M. L., Parsadanian, A. S., Doster, K., Wen, D., Yan, Q. and Snider, W. D. (1997). IB4-binding DRG neurons switch from NGF to GDNF dependence in early postnatal life. *Neuron* **19**, 849-861.

Oppenheim, R. W., Houenou, L. J., Johnson, J. E., Lin, L. F., Li, L., Lo, A. C., Newsome, A. L., Prevette, D. M. and Wang, S. (1995). Developing motor neurons rescued from programmed and axotomy-induced cell death by GDNF. *Nature* **373**, 344-346. doi:10.1038/373344a0

Paratcha, G. and Ledda, F. (2008). GDNF and GFRalpha: a versatile molecular complex for developing neurons. *Trends Neurosci.* **31**, 384-391. doi:10.1016/j.tins.2008.05.003

Paratcha, G., Ledda, F., Baars, L., Coulpier, M., Besset, V., Anders, J., Scott, R. and Ibanez, C. F. (2001). Released GFRalpha1 potentiates downstream signaling, neuronal survival, and differentiation via a novel mechanism of recruitment of c-Ret to lipid rafts. *Neuron* **29**, 171-184.

Park, H. J. and Bolton, E. C. (2017). RET-mediated glial cell line-derived neurotrophic factor signaling inhibits mouse prostate development. *Development* **144**, 2282-2293.

Paveliev, M., Airaksinen, M. S. and Saarma, M. (2004). GDNF family ligands activate multiple events during axonal growth in mature sensory neurons. *Mol. Cell. Neurosci.* **25**, 453-459. doi:10.1016/j.mcn.2003.11.010

Powell, A. E., Wang, Y., Li, Y., Poulin, E. J., Means, A. L., Washington, M. K., Higginbotham, J. N., Juchheim, A., Prasad, N., Levy, S. E. et al. (2012). The pan-ErbB negative regulator Lrig1 is an intestinal stem cell marker that functions as a tumor suppressor. *Cell* **149**, 146-158. doi:10.1016/j.cell.2012.02.042

Rafidi, H., Mercado, F., III, Astudillo, M., Fry, W. H. D., Saldana, M., Carraway, K. L., III and Sweeney, C. (2013). Leucine-rich repeat and immunoglobulin domain-containing protein-1 (Lrig1) negative regulatory action toward ErbB receptor tyrosine kinases is opposed by leucine-rich repeat and immunoglobulin domain-containing protein 3 (Lrig3). *J. Biol. Chem.* **288**, 21593-21605. doi:10.1074/jbc.M113.486050

Sakai, K., Sanders, K. M., Youssef, M. R., Yanushefski, K. M., Jensen, L. E., Yosipovitch, G. and Akiyama, T. (2017). Role of neurturin in spontaneous itch and increased nonpeptidergic intraepidermal fiber density in a mouse model of psoriasis. *Pain* **158**, 2196-2202. doi:10.1097/j.pain.0000000000001025

Sergaki, M. C., Lopez-Ramos, J. C., Stagkourakis, S., Gruart, A., Broberger, C., Delgado-Garcia, J. M. and Ibanez, C. F. (2017). Compromised survival of cerebellar molecular layer interneurons lacking GDNF Receptors GFRalpha1 or RET impairs normal cerebellar motor learning. *Cell Rep* **19**, 1977-1986. doi:10.1016/j.celrep.2017.05.030

Shattuck, D. L., Miller, J. K., Laederich, M., Funes, M., Petersen, H., Carraway, K. L., III and Sweeney, C. (2007). LRIG1 is a novel negative regulator of the Met receptor and opposes Met and Her2 synergy. *Mol. Cell. Biol.* **27**, 1934-1946. doi:10.1128/MCB.00757-06

Song, M., Giza, J., Proenca, C. C., Jing, D., Elliott, M., Dincheva, I., Shmelkov, S. V., Kim, J., Schreiner, R., Huang, S. H. et al. (2015). Slitrk5 mediates BDNF-dependent TrkB receptor trafficking and signaling. *Dev. Cell* **33**, 690-702. doi:10.1016/j.devcel.2015.04.009

Suzuki, Y., Miura, H., Tanemura, A., Kobayashi, K., Kondoh, G., Sano, S., Ozawa, K., Inui, S., Nakata, A., Takagi, T. et al. (2002). Targeted disruption of LIG-1 gene results in psoriasiform epidermal hyperplasia. *FEBS Lett.* **521**, 67-71. doi:10.1016/S0014-5793(02)02824-7

Treanor, J. J., Goodman, L., de Sauvage, F., Stone, D. M., Poulsen, K. T., Beck, C. D., Gray, C., Armanini, M. P., Pollock, R. A., Hefti, F. et al. (1996). Characterization of a multicomponent receptor for GDNF. *Nature* **382**, 80-83. doi:10.1038/382080a0

Trupp, M., Arenas, E., Fainzilber, M., Nilsson, A. S., Sieber, B. A., Grigoriou, M., Kilkenny, C., Salazar-Grueso, E., Pachnis, V. and Arumae, U. (1996). Functional receptor for GDNF encoded by the c-ret proto-oncogene. *Nature* **381**, 785-789. doi:10.1038/381785a0

Wang, T., Jing, X., DeBerry, J. J., Schwartz, E. S., Molliver, D. C., Albers, K. M. and Davis, B. M. (2013). Neurturin overexpression in skin enhances expression

of TRPM8 in cutaneous sensory neurons and leads to behavioral sensitivity to cool and menthol. *J. Neurosci.* **33**, 2060-2070.

Wong, V. W., Stange, D. E., Page, M. E., Buczacki, S., Wabik, A., Itami, S., van de Wetering, M., Poulsom, R., Wright, N. A., Trotter, M. W. et al. (2012). Lrig1 controls intestinal stem-cell homeostasis by negative regulation of ErbB signalling. *Nat. Cell Biol.* **14**, 401-408.

Yan, H., Newgreen, D. F. and Young, H. M. (2003). Developmental changes in neurite outgrowth responses of dorsal root and sympathetic ganglia to GDNF, neurturin, and artemin. *Dev. Dyn.* **227**, 395-401. doi:10.1002/dvdy.10294

Zhao, H., Tanegashima, K., Ro, H. and Dawid, I. B. (2008). Lrig3 regulates neural crest formation in Xenopus by modulating Fgf and Wnt signaling pathways. *Development* **135**, 1283-1293. doi:10.1242/dev.015073

Zimmermann, K., Leffler, A., Babes, A., Cendan, C. M., Carr, R. W., Kabayashi, J., Nau, C., Wood, J. N. and Reeh, P. W. (2007). Sensory neuron sodium channel Nav1.8 is essential for pain at low temperatures. *Nature* **447**, 855-859. doi:10.1038/nature05880

Zwick, M., Davis, B. M., Woodbury, C. J., Burkett, J. N., Koerber, H. R., Simpson, J. F. and Albers, K. M. (2002). Glial cell line-derived neurotrophic factor is a survival factor for isolectin B4-positive, but not vanilloid receptor 1-positive, neurons in the mouse. *J. Neurosci.* **22**, 4057-4065.

Zylka, M. J., Rice, F. L. and Anderson, D. J. (2005). Topographically distinct epidermal nociceptive circuits revealed by axonal tracers targeted to Mrgprd. *Neuron* **45**, 17-25. doi:10.1016/j.neuron.2004.12.015

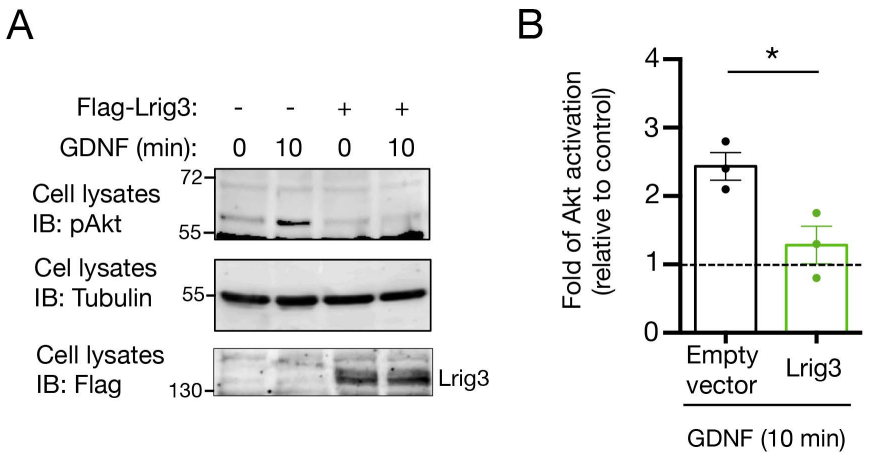

Fig. S1. Lrig3 inhibits GDNF-induced Akt activation

(A) Representative immunoblotting of Akt activation in cell extracts prepared from MN1 cells transfected with empty vector or Flag-Lrig3 constructs. Cells were treated with GDNF (50 ng/ml) as indicated. Akt phosphorylation was normalized with the signal intensity of tubulin. Expression of Flag-Lrig3 in total cell extracts is also shown.

(B) Bar graph shows the quantification of Akt activation. Results are presented as fold of change of Akt activation relative to control untreated samples (dotted line). Data are presented as average ± SEM from three independent experiments. *$p<0.05$ by two-tailed Student's test.

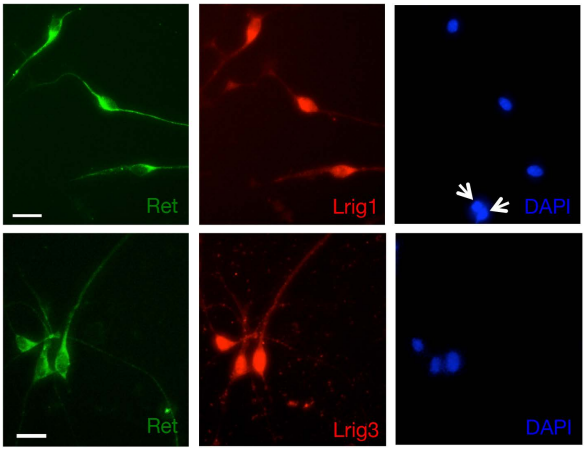

Fig. S2. Co-expression of Lrig1 and Lrig3 with Ret in DRG primary neurons
Localization by immunofluorescence of Lrig1 (top, red), Lrig3 (bottom, red), and Ret (green) in DRG-dissociated neurons. Arrowheads indicate cells negative for Ret and Lrig1. Scale bars, 20μm.

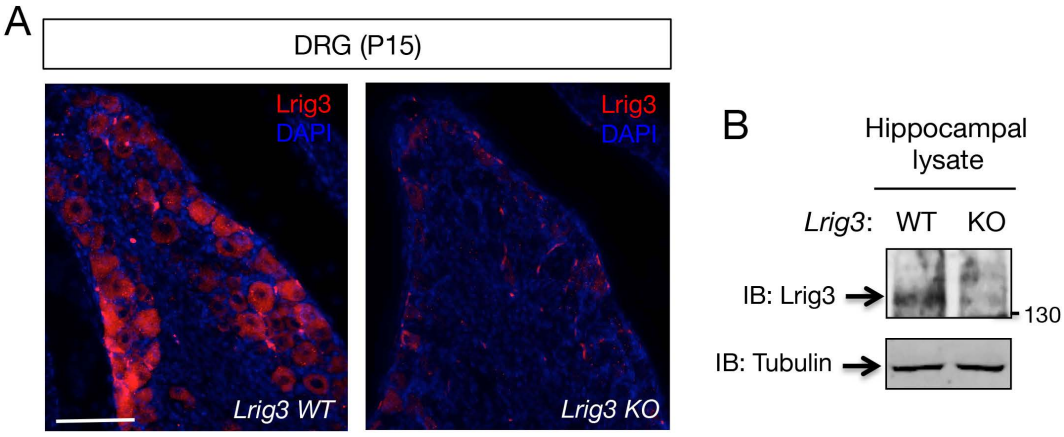

Fig. S3. Control of anti-Lrig3 antibody (mLrig3 207) specificity

(A) Confocal images of Lrig3 immunofluorescence on DRG lumbar sections obtained from P15 wild-type and *Lrig3*-deficient mice. Scale bar, 100 μm.
(B) Antibody specificity was additionally confirmed by immunoblotting (IB) analysis of hippocampal homogenates obtained from wild-type and *Lrig3* knockout mice. Protein loading was controlled by tubulin expression.

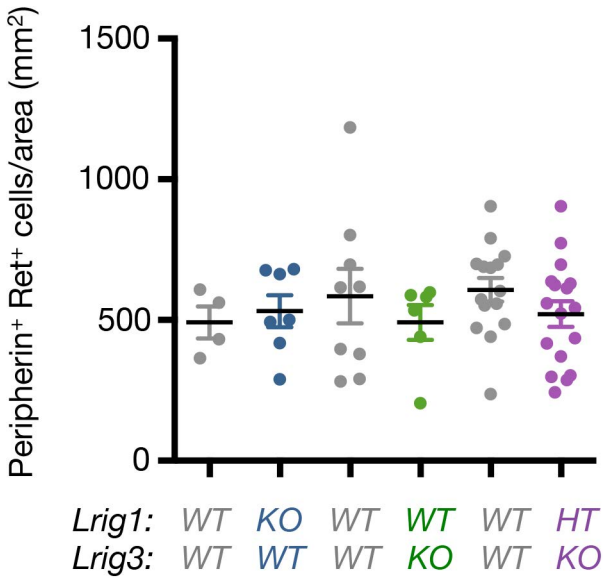

Fig. S4. Nonpeptidergic nociceptive (Peripherin+/Ret+) neuronal cell density is not affected in *Lrig1KO*, *Lrig3KO* and *Lrig1HT/Lrig3KO* mice

Graph shows the average of Peripherin+/Ret+ nonpeptidergic neuronal cell density in lumbar DRG sections isolated from P15 wild-type (n=28 ganglia), *Lrig1KO* (n=7 ganglia), *Lrig3KO* (n=6 ganglia) and *Lrig1HT/Lrig3KO* (n=17 ganglia) mice. Each mutant genotype is presented with its corresponding WT littermate control. $p>0.05$ by ANOVA

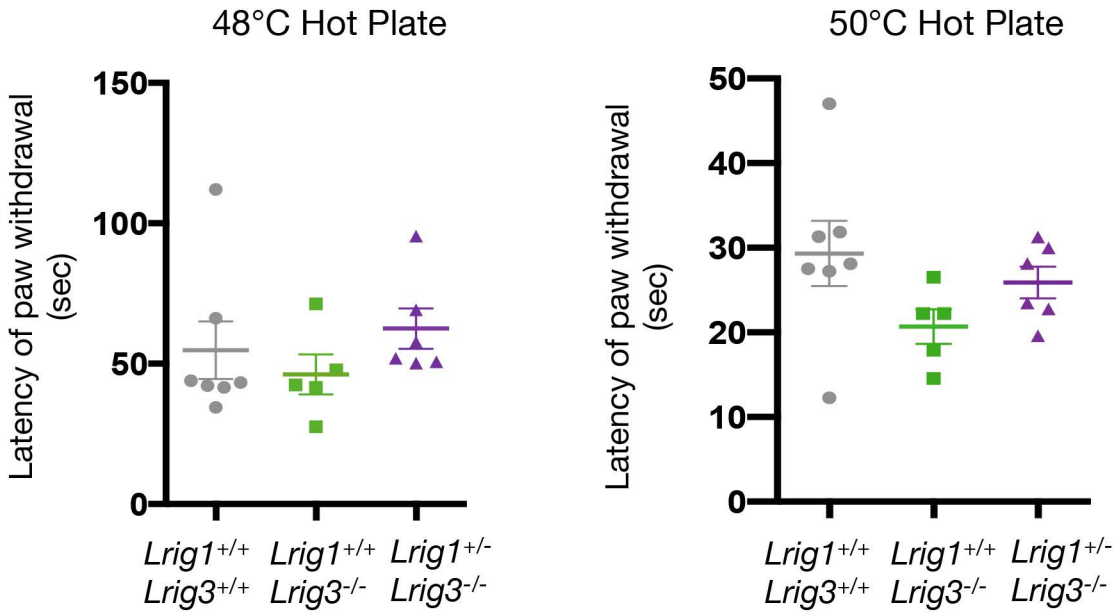

Fig. S5. *Lrig3KO* and *Lrig1HT/Lrig3KO* mice do not show differential behavioral response in the hot plate test

Graphs show individual values of the latency time (sec) of paw withdrawal of *Lrig1WT/Lrig3WT* (n=7), *Lrig1WT/Lrig3KO* (n=5) and Lrig1HT/Lrig3KO (n=6) mice in the hot platetest at the indicated temperatures. Each graph shows the means ± SEM. $p>0.05$ by ANOVA